1 *Article*

2 # Effects of Periostracum Cicadae on Cytokines and Apoptosis
3 # Regulatory Proteins in IgA Nephropathy Rat Model

4 **Lu Yang[1, 2], Yan Wang[1,2], Aobulikasimu·NUERBIYE[3], Ping Cheng [1,2], Jin-Hui Wang [3,4],**
5 **RENA Kasimu[3] and Hong Li [1] ***

6 [1] Xinjiang Academy of Forestry, Urumqi 830000, China; yanglukitty127@163.com(L.Y.);
7   18999537981@163.com(Y.W.); chengping1985@163.com(P.C.);

8 [2] Economic forest product quality inspection and testing center of the State Forestry Administration
9   (Urumqi), Urumqi 830052, China;

10 [3] Xinjiang Medical University, Urumqi 830000, China; renakasimu@vip.sina.com

11 [4] Harbin Medical University, Harbin 150081, China; tcm_shz@aliyun.com

12 * Correspondence: xjlky_sys@163.com; Tel.: +188-9916-1201

13

14 **Abstract** Periostracum cicadae, the cast-off shell of the cicada *Cryptotympana pustulata* Fabricius, is
15 used in traditional Chinese medicine for its diaphoretic, anticonvulsive, sedative, antipyretic, and
16 antiallergic effects. However, the exact pathogenesis of immunoglobulin A nephropathy (IgAN)
17 remains unclear, thereby hindering investigations to identify novel therapeutic agents. A rat IgAN
18 model was established by administration of bovine serum albumin, lipopolysaccharide, and carbon
19 tetrachloride, which simultaneously established blood stasis and a heat syndrome model. The
20 animals were sacrificed to detect changes in protein levels in urine and blood. Immunofluorescence
21 was performed to assess IgA deposition in the glomeruli. Tumor necrosis factor-α (TNF-α),
22 interleukin-1β (IL-1β), and interleukin 6 (IL-6) levels were measured in bronchoalveolar lavage fluid
23 (BALF) by enzyme-linked immunosorbent assay. Hematology and eosin, periodic acid-Schiff,
24 TUNEL, and immunohistochemical staining were performed to evaluate histopathological changes
25 in kidney tissues. Additionally, target-related proteins were measured by western blotting.
26 Periostracum cicadae resulted in a reduction in blood and urine protein levels. Serum TNF-α, IL-1β,
27 and IL-6 levels significantly decreased in the periostracum cicadae-treated groups compared to the
28 IgAN group. Furthermore, a reduction in MCP-1, TLR4, and IgA expression levels and a dose-
29 dependent increase in caspace-3 expression were observed in response to periostracum cicadae
30 treatment. TGF-β1 levels decreased, whereas that of Fas increased in the kidney tissues of the
31 periostracum cicadae-treated groups. The findings of the present study indicate that periostracum
32 cicadae induces apoptosis and improves kidney inflammation and fibrosis in IgA nephropathy rat
33 models.

34 **Keywords:** Periostracum cicadae; IgA nephropathy; inflammation; fibrosis; apoptosis

35

36 ## 1. Introduction

37   Immunoglobulin A nephropathy (IgAN) is the most common type of glomerulonephritis in the world
38 [1]. IgA nephropathy is characterized by immune deposits predominantly composed of polymeric
39 IgA in the glomerular mesangium [2-5]. Nephrotic-range proteinuria, microscopic hematuria and renal
40 failure impairment are strong predictors of an adverse clinical outcome[6-8]. The risk of progression to

41 chronic kidney disease in patients with IgAN in adults is apparently significantly higher in children.
42 IgAN patients with proteinuria are generally considered to have increased risk for progression to chronic
43 kidney disease (CKD) and renal failure [9]. Renal involvement is the most serious long-term
44 complication; its symptoms include asymptomatic microhematuria and/or mild proteinuria to overt
45 IgAV nephritis (IgAVN)[10]. IgAVN, which occurs in approximately 30% of pediatric patients within
46 4–6 weeks of initial presentation [11], and severe IgAVN are both associated with decreased renal
47 function, hypertension, hypoalbuminemia, and long-term renal sequelae. Current treatment for
48 IgAVN, which include steroids and immunosuppressive drugs, are mainly based on the findings of
49 studies on IgAN [12]. Recently, Oxford presented a new classification for IgA nephropathy as
50 proposed by a Working Group of the International IgA Nephropathy Network and the Renal
51 Pathology Society [13], which has been validated by numerous studies [14-18]. This group identified
52 four histopathologic features that are associated with the progression of kidney disease: mesangial
53 hypercellularity score (M; M0 ≤0.5, M1 ≥0.5), the presence of endocapillary proliferation (E; E0: absent,
54 E1: present), segmental glomerulosclerosis/adhesion (S; S0: absent, S1: present), and the severity of
55 tubular atrophy/interstitial fibrosis (T; T0 ≤25%, T1: 26%–50%, T2 ≥50%). However, the exact
56 pathogenesis of IgAN remains unclear, thereby hindering research investigations to identify novel
57 therapeutic agents for the treatment of this particular disease.

58 The traditional Chinese crude drug periostracum cicadae is the cast-off shell of Cryptotympana
59 pustulata Fabricius, commonly known as the black cicada. Periostracum cicadae has a sweet and salty
60 taste and produces a 'cooling' effect. Periostracum cicadae is known as chantui in traditional Chinese
61 medicine and has been historically used in the treatment of sore throat, hoarseness, itching, spasms,
62 and other symptoms. The crude extract of periostracum cicadae can be used as a sedative,
63 hypothermic, anticonvulsive [19], antioxidant, anti-inflammatory [19-20], antipyretic, and antiallergic
64 agent [21], as well as a sympathetic ganglionic blocker [22] when administered by various routes. To
65 our knowledge, this is the first study that has investigated the molecular mechanism of periostracum
66 cicadae in inflammation and fibrosis using an IgAN model.

67 **2. Results**

68 *2.1. The effect of periostracum cicadae on proteinuria and other biochemical parameters*

69 We examined the physical appearance and biochemical parameters of the rats. The IgAN rats
70 showed gray hair, slow growth and reduced amount of activity. After molding, collecting 24 hours
71 of urine from rats, and observing that IgAN rats developed macroscopic hematuresis, however
72 normal group and treatment group had no expression. The IgAN rat models showed significantly
73 higher urine protein, blood urea nitrogen (BUN), and serum creatinine (Src) levels than the normal,
74 healthy controls, whereas these were markedly lower in the treatment group (Figure 1). These
75 findings indicate that periostracum cicadae treatment lowers protein, BUN, and CREA levels in the
76 IgAN rat model.

77 Figure 2 shows that serum alanine amino transferase (ALT), aspartate aminotransferase (AST),
78 total protein (TP), ALB, GLOB, BUN, TCHO1, CREA, and TG levels significantly increased in the
79 IgAN rat models compared to normal, healthy controls, whereas serum ALT, AST, TP, ALB, GLOB,
80 BUN, TCHO1, CREA, and TG levels dramatically decreased in the periostracum cicadae treatment
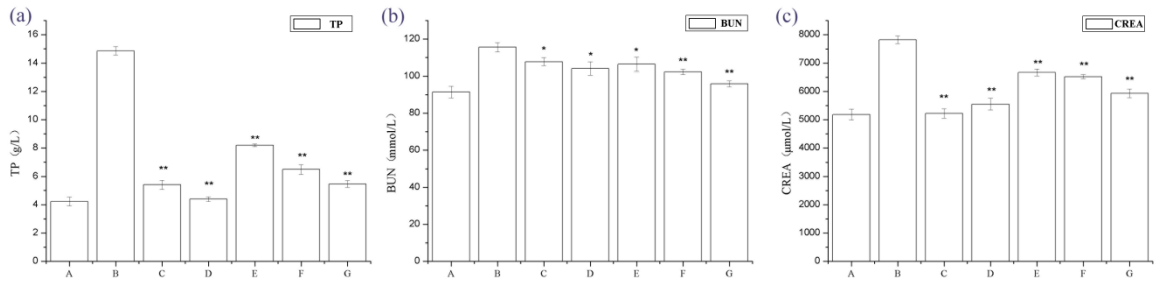81 group compared to the IgAN model group.

Figure 1. Changes in 24-h urine protein, blood urea nitrogen (BUN), and serum creatinine (Scr) levels. *P < 0.05,**P < 0.01 compared to the IgAN model group. (A) normal, healthy controls; (B) IgAN rat models; (C) prednisone acetate group (PAG); (D) tripterygium glycoside tablet group; (E–G) treatment group that received 0.5 g/kg, 1 g/kg, and 2 g/kg periostracum cicadae, respectively.
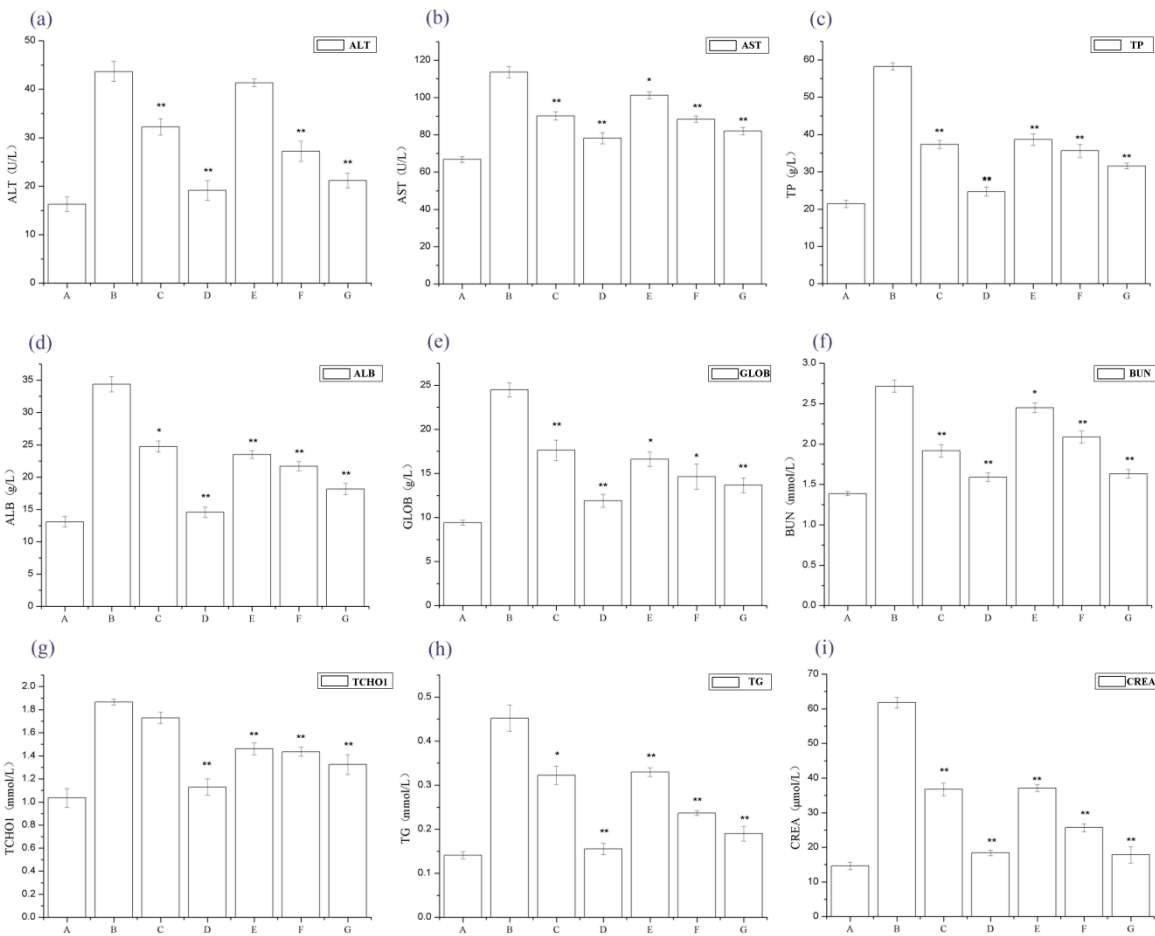

Figure 2. Changes in serum alanine aminotransferase (ALT), aspartate aminotransferase (AST), total protein (TP), total cholesterol (TCHO), triacylglyceride (TAG), BUN and CREA levels. *P < 0.05,**P < 0.01 compared to the IgAN model group. (A) normal, healthy controls; (B) IgAN model group; (C) prednisone acetate group; (D) tripterygium glycoside tablet group; (E–G) treatment group that received 0.5 g/kg, 1 g/kg, and 2 g/kg periostracum cicadae, respectively.

2.2. The effect of periostracum cicadae on IgA

To evaluate the effects of periostracum cicadae on IgA levels, we measured serum IgA levels by ELISA (Figure 3a). The IgA levels of the model group were significantly higher compared to the untreated control group, whereas these were significantly lower in the treatment group relative to the model group.

98   IgA deposits in the glomeruli were observed by immunofluorescence staining (Figure 3b). The
99   control rats showed minimal IgA deposition in the glomeruli, with an average fluorescence intensity
100 of "−" (Table 1). In contrast, the IgAN rats exhibited significant mass- or granule-like red fluorescence
101 that was scored as "+" to "++++"; however, these images did not provide evidence for increased
102 deposition in the thick loop region. The majority of the fluorescence was observed in the glomeruli.
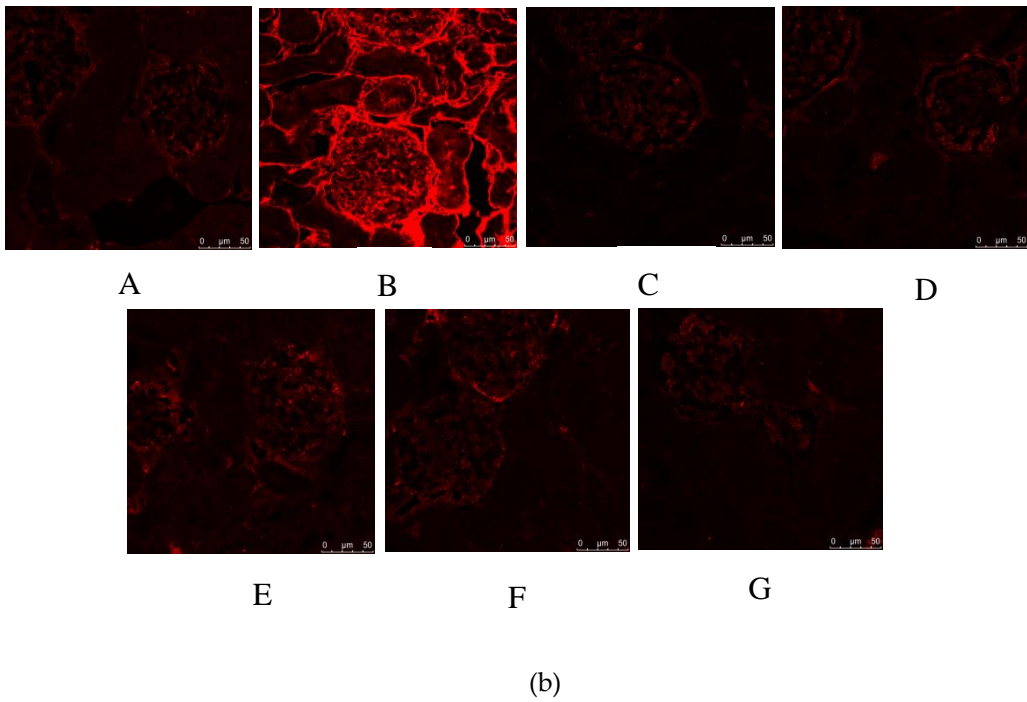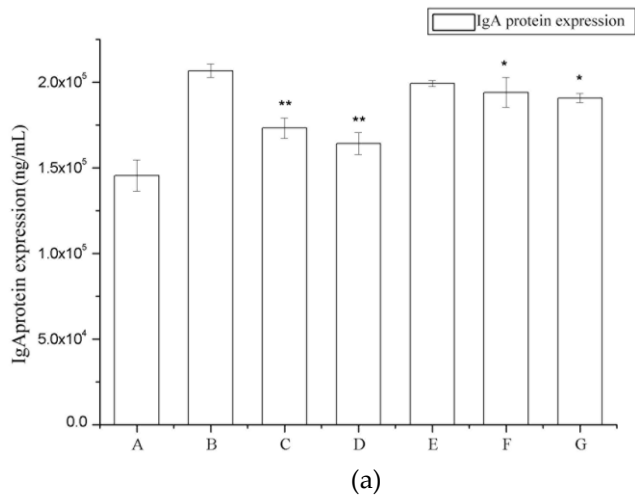103 These findings were indicative that the IgAN animal model was successfully established.

104

(a)

105

106   (b)

107 **Figure 3.** The effect of periostracum cicadae on IgA deposition. (a) Effects of periostracum cicadae on serum IgA
108 levels in IgAN rats. (*P < 0.05,**P < 0.01). (b) Immunofluorescence staining of IgA in the glomeruli (A) normal,
109 healthy controls; (B) IgAN model group; (C) prednisone acetate group; (D) tripterygium glycoside tablet group;
110 (E–G) treatment group that received 0.5 g/kg, 1 g/kg, and 2 g/kg periostracum cicadae.

111   **Table 1.** IgA fluorescence intensities

Group	controls	IgAN model group	Prednisone acetate group	tripterygium glycoside tablet group	Periostracum cicadae group

				0.5 g/kg	1 g/kg	2 g/kg
IgA deposits	−	++++	+	++	+++	++	+

2.3. Periostracum cicadae alleviates inflammation in rats with IgAN

To determine the effect of periostracum cicadae on the renal inflammatory responses of rats, the serum levels of the inflammatory cytokines TNF-α, IL-1β, and IL-6 were evaluated. The serum TNF-α, IL-1β and IL-6 levels of the IgAN model group significantly increased compared to those in the untreated control group, whereas those of the treatment group were significantly lower than the IgAN model group (Figure 4). These data show that periostracum cicadae treatment lowers serum TNF-α, IL-1β, and IL-6 levels, indicating that periostracum cicadae has anti-inflammatory properties that alleviate IgAN-induced kidney fibrosis in rats.
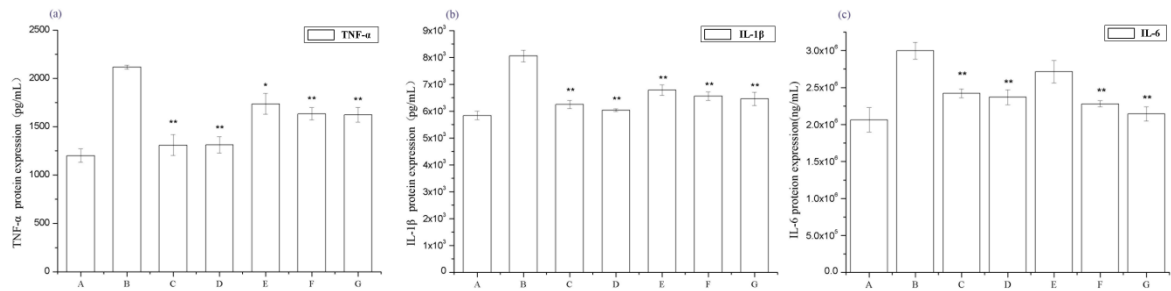

Figure 4. Effects of periostracum cicadae on the serum levels of tumor necrosis factor-α (TNF-α), interleukin-1β (IL-1β), and interleukin 6 (IL-6) in IgAN rats. (*P < 0.05,**P < 0.01). (A) Healthy, normal control group; (B) IgAN model group; (C) prednisone acetate group; (D) tripterygium glycoside tablet group; (E–G) treatment group that received 0.5 g/kg, 1 g/kg, and 2 g/kg periostracum cicadae, respectively.

### 2.4. The effect of periostracum cicadae on inflammatory cell infiltration

Asthmatic mice that received periostracum cicadae were histopathologically evaluated using hematoxylin and eosin (H&E) (Figure 5a) and PAS (Figure 5b) staining. In the untreated control group (Figure 5a), the kidneys were broad, bean-shaped, shiny, and reddish-brown in color. No changes in the organization of the glomeruli and renal tubules were observed. The renal tissue structures were intact and well organized, the glomeruli showed normal size, the renal tubules did not depict any signs of swelling or degeneration, and the interstitial regions did not exhibit inflammatory cell infiltration or fibrosis. The renal tubular epithelial cells were normal in size and the distal tubules did not show any detectable signs of expansion. A few transparent tubules in the renal tubules were observed, and no significant inflammatory cell infiltration in the stroma was detected. In the model group, glomerular hypertrophy, renal interstitium edema and a mass of inflammatory cell infiltration and fibrosis revealed in the interstitial regions were researched. The prednisone acetate and tripterygium glycoside tablet treatment groups illustrated that The glomerular size was slightly larger, existing a spot of inflammatory cell infiltration. The kidneys of the periostracum cicadae group showed a significant increase in size, dark red in color, with a small amount of inflammatory cell infiltration.

In the untreated control group (Figure 5b), no proliferative glomerular basilar membrane, mesangium or glomerular sclerosis was observed. In the model group, hyperplasia of glomerular mesenterium and basilar membrane tubular, swelling accompanied by segmental glomerulosclerosis, collapsed glomerular vascular loops, and perivascular inflammatory cell infiltration were observed. The prednisone acetate and tripterygium glycoside tablet treatment groups showed proliferative glomerular mesangium and basilar membrane were unconspicuous, with minimal inflammatory cell

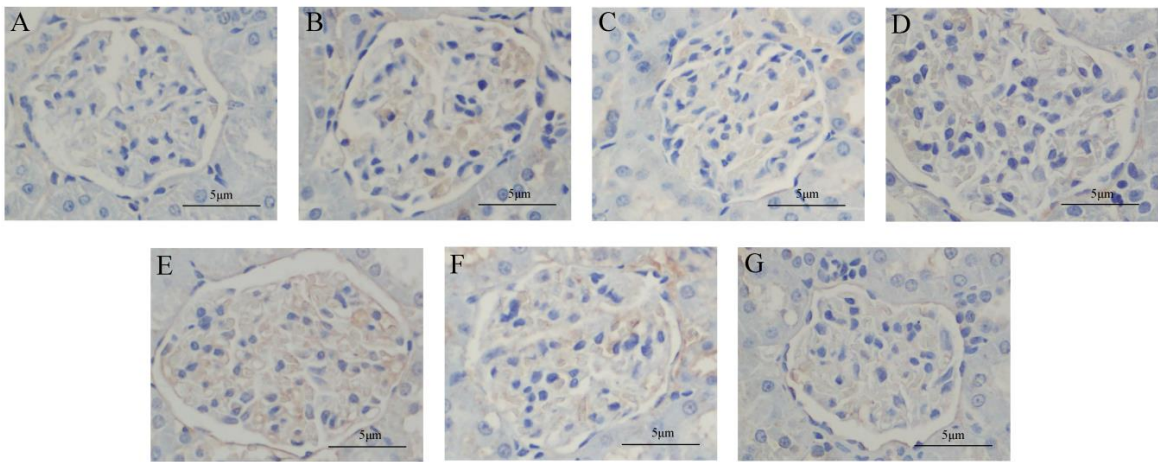148 infiltration. The periostracum cicadae treatment group exhibited mesangial thickening, but was
149 better than the model group, as well as a small number of inflammatory cell infiltration.

150

151

(a)

152

153

(b)

154

155

(c)
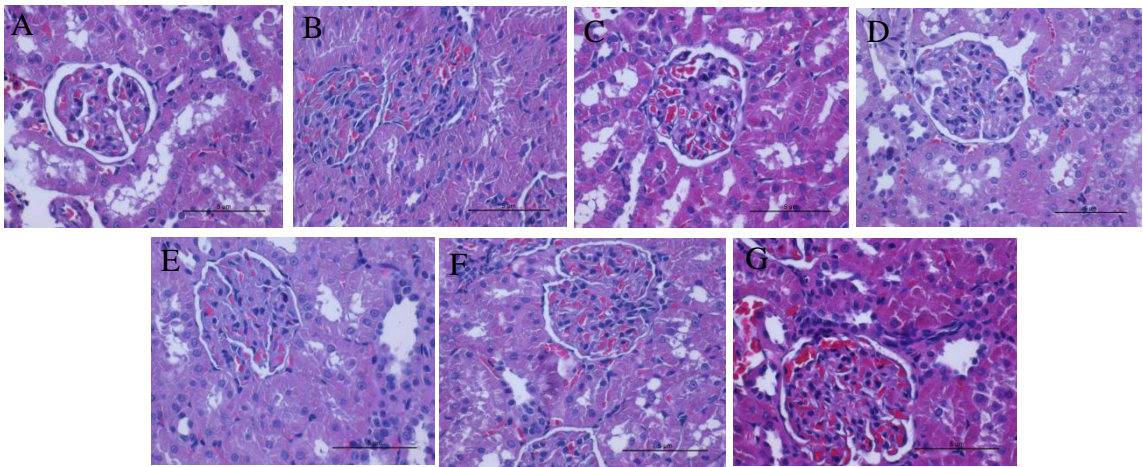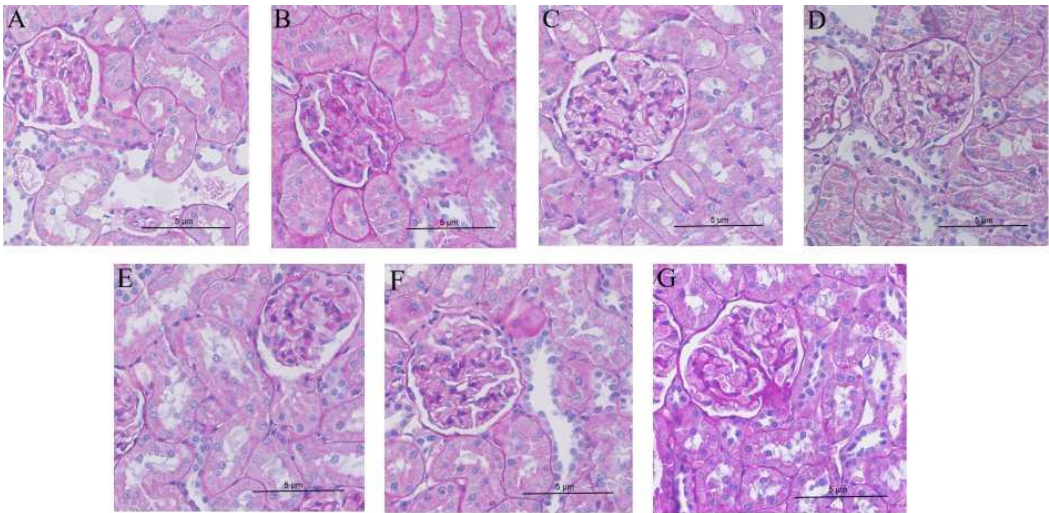
156   **Figure 5.** Periostracum cicadae improves kidney inflammation and fibrosis and induces cell apoptosis.
157   (a) Hematoxylin and eosin (H&E) staining. (b) Periodic acid-Schiff (PAS) staining. (c) TdT-mediated
158   dUTP nick end-labeling (TUNEL) staining.

159   *2.5. Periostracum cicadae induces cellular apoptosis in the IgAN rat model*

160   To gain insights on whether periostracum cicadae induces apoptosis in vivo, paraffin sections
161   from the Sprague-Dawley (SD) rats were subjected to H&E staining (Figure 5a). The increase in the
162   number of TdT-mediated dUTP nick end-labeling (TUNEL)-positive cells clearly demonstrates that
163   cellular apoptosis was detected (Figure 5c). The microscopic signs of cellular apoptosis showed that
164   cellular shrinkage, condensed, bright eosinophilic cytoplasm and pyknotic small, dark nuclei were
165   demonstrated due to chromatin condensation. Figure 5a and Figure 5c showed no chromatin
166   condensation and normal cell size in the untreated control group. In the model group, chromatin
167   condensation, apoptosis of glomerular epithelial cells were examined. The prednisone acetate and
168   tripterygium glycoside tablet treatment groups indicated apoptosis of inflammatory cells were rare.
169   The result of coloration selecting TUNEL in the periostracum cicadae treatment group clearly
170   demonstrates that periostracum cicadae induces inflammatory cellular apoptosis in vivo.

171   *2.6. The effect of periostracum cicadae on TGF-β1- and Fas-positive cells*

172   Figure 6a shows that a region of the glomeruli was positively immunostained for TGF-β1,
173   whereas this was not observed in the saline-treated group; a larger TGF-β1 immunostained area was
174   observed in the model group (Figure 6a) and a smaller area was detected in the periostracum cicadae
175   treatment group using doses of 0.5 g/kg/day, 1.0 g/kg/day, and 2.0 g/kg/day. The prednisone acetate
176   and tripterygium glycoside tablet treatment groups showed a significant increase in the TGF-β1-
177   positive area within the glomeruli. Immunohistochemical staining of kidney sections showed that
178   prednisone acetate significantly decreased the secretion of TGF-β1 in rats with IgAN (P <0.05, P <0.01
179   *vs*. IgAN model group; Figure 6b). Consistent with the immunohistochemical staining results, ELISA
180   also revealed a suppressive effect of periosteacum cicadae on TGF-β1 expression (Figure 6c).

181   The number of Fas-positive cells in the IgAN rats was lower compared to that in the saline-
182   treated group (Figure 7a). The periostracum cicadae treatment group showed an increase in the
183   number of Fas-positive cells. Figure 7b shows that prednisone acetate induces a marked increase in
184   FAS expression (P< 0.01), whereas that in the IgAN group was significantly lower than in the normal,
185   healthy control group and increased in a dose-dependent manner after periostracum cicadae
186   administration. The FAS levels determined by ELISA in the model group were lower compared to
187   the untreated control group, whereas the levels were significantly induced in the treatment group
188   relative to that in the model group (Figure 7c).
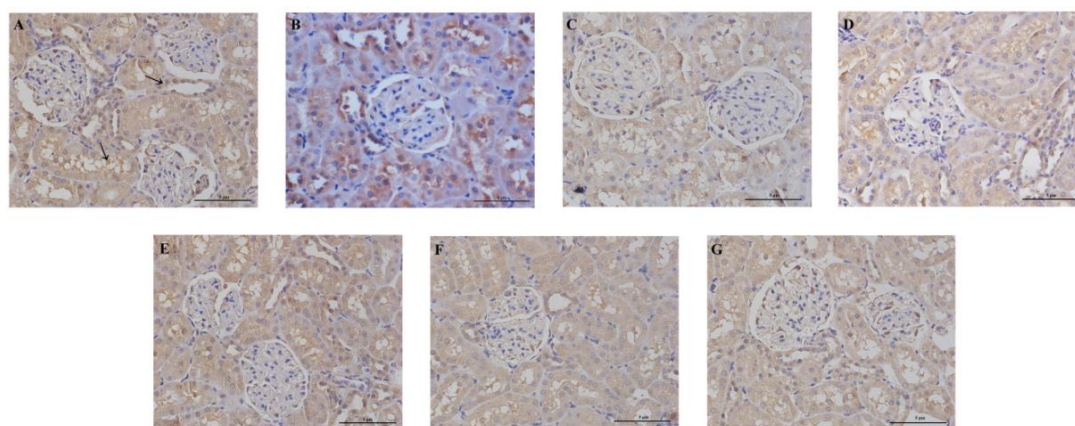
189
190   (a)
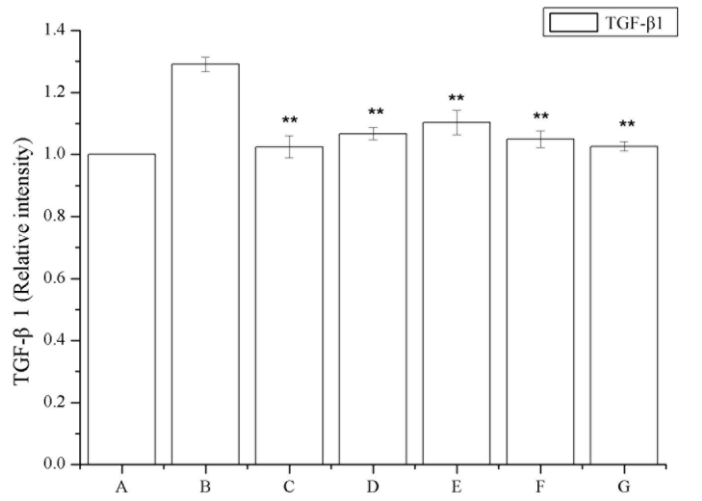
(b)
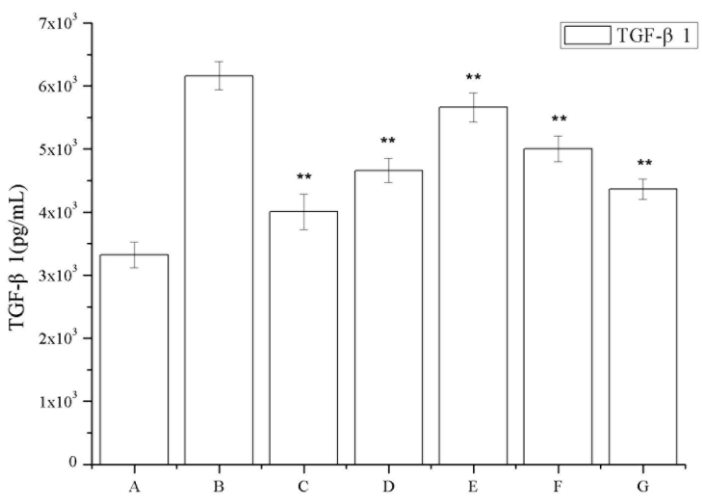
(c)

Figure 6. Effects of periostracum cicadae on the levels of TGF-β1 in the kidney. (a) representative immunohistochemistry image (A) normal, healthy control group; (B) IgAN model group; (C) prednisone acetate group; (D) tripterygium glycoside tablet group; (E–G) treatment group that received 0.5 g/kg, 1 g/kg, and 2 g/kg periostracum cicadae; (b) the quantitative analysis of TGF-β1 protein in kidney tissues. Data represent the mean ± standard deviation(*P < 0.05,**P < 0.01 *vs* model group); (c) effects of periosteacum cicadae on the levels of TGF-β1 in the tissue of IgAN rats. (*P < 0.05,**P < 0.01)
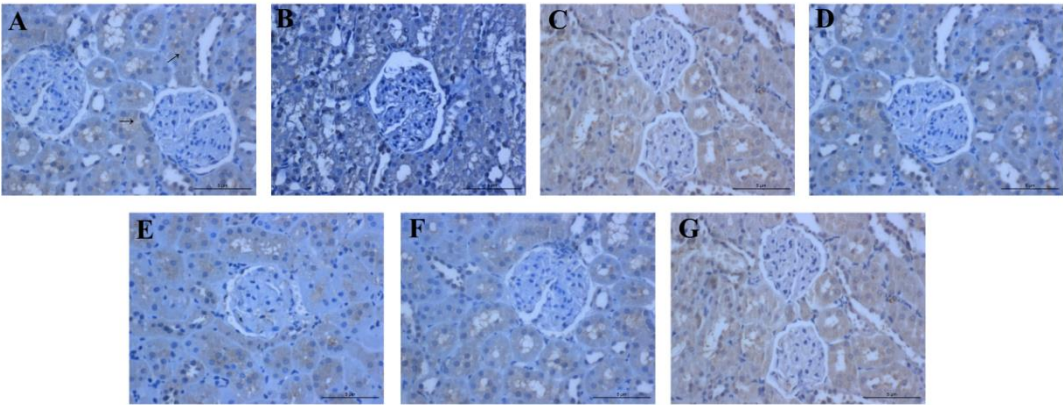
(a)

(b)
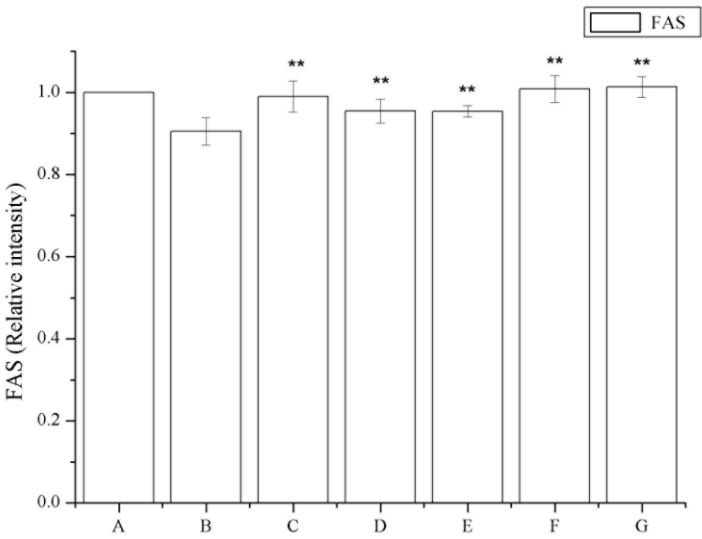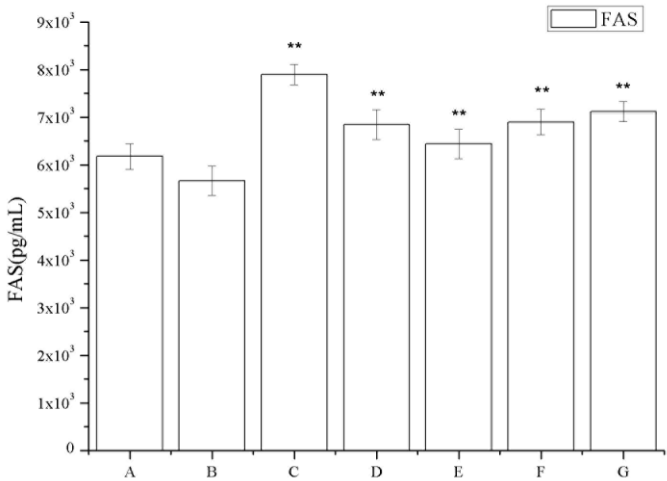

(c)

Figure 7. Effects of periostracum cicadae on FAS levels in the kidney. (a) representative immunohistochemistry image (A) normal, healthy control group; (B) IgAN model group; (C) prednisone acetate group; (D) tripterygium glycoside tablet group; (E–G) treatment group that

211   received 0.5 g/kg, 1 g/kg, and 2 g/kg periostracum cicadae; (b) the quantitative analysis of FAS protein
212   in kidney tissues. Data represent the mean ± standard deviation(*P < 0.05,**P < 0.01 *vs* model group);
213   (c) effects of periosteacum cicadae on the levels of FAS in the tissue of IgAN rats. (*P < 0.05,**P < 0.01)

214   *2.7. Assessment of TLR4, MCP-1, IgA, and caspase 3 expression levels*

215   The levels of MCP-1, TLR4, IgA, and caspase 3 expression were investigated by western blotting,
216   using β-actin for normalization. A significant inhibition of TLR4, MCP-1, and IgA expression in the
217   periostracum cicadae-treated rats was observed relative to that in the model group. The expression
218   of TLR4, MCP-1, and IgA was significantly lower in the periostracum cicadae-treated rats than that
219   in the model group. Figure 8 shows that the normal, healthy controls exhibited lower TLR4, MCP-1,
220   and IgA expression levels, whereas these were significantly higher in the IgAN groups. However,
221   after periostracum cicadae treatment, TLR4, MCP-1, and IgA expression gradually decreased. These
222   findings suggest that periostracum cicadae treatment mitigates MCP-1, TLR4, and IgA expression in
223   the IgAN rats. The untreated control group exhibited a relatively higher caspase 3 expression level
224   than the IgAN groups. However, after periostracum cicadae treatment, caspase 3 expression
225   gradually increased. Caspase 3 activity is an integral step in most apoptotic events. In the present
226   study, treatment with periostracum cicadae resulted in the upregulation of caspase 3. These results
227   show that periostracum cicadae plays a key role in inducing apoptosis in IgAN rats.

228

229   (a)

230

231   (b)
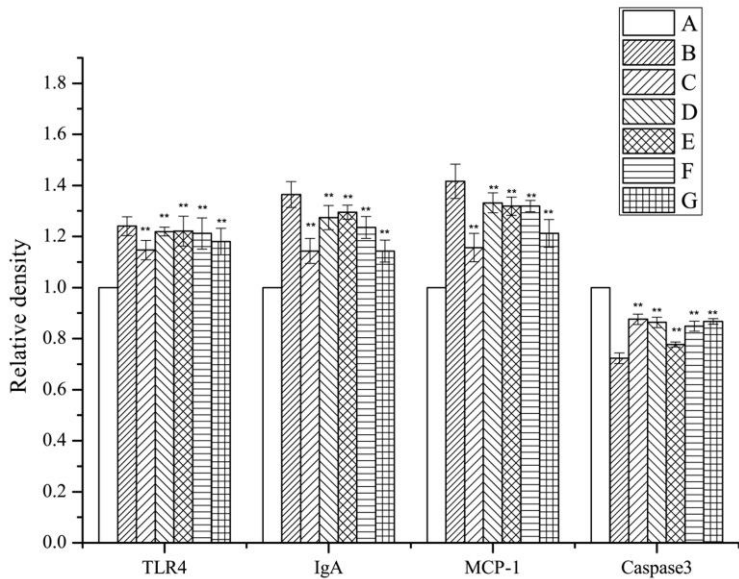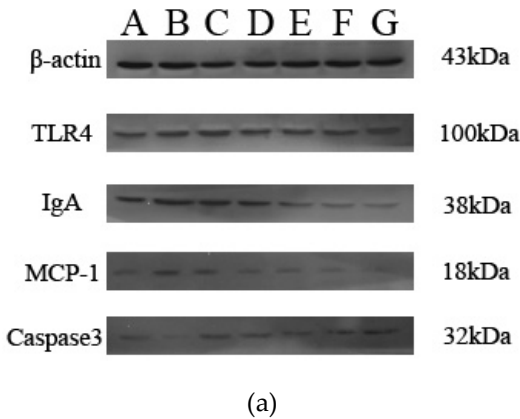
232   **Figure 8.** TLR4, MCP-1, IgA, and caspase-3 expression in rat kidney tissues. (a) TLR4, IgA, MCP-1,
233   and caspase-3 expression levels were analyzed by western blotting. (b) Quantitative analysis of TLR4,

234   IgA, MCP-1, and caspase-3 protein levels. (A) healthy, normal controls; (B) IgAN model group; (C)
235   prednisone acetate group; (D) tripterygium glycoside tablet group; (E–G) treatment group that
236   received 0.5 g/kg, 1 g/kg, and 2 g/kg periostracum cicadae.

3. Discussion

238   IgA nephropathy is characterized by increased levels of galactose-deficient IgA1 (Gd-IgA1) that
239   is complicated by nephritis, and Gd-IgA1 is now believed to play a pivotal role in the pathogenesis
240   of both IgA nephropathy. In addition, IgA-containing complexes have been found in the glomeruli
241   of IgA nephropathy and IgAN patients. IgA nephropathy can damage the liver, M Zaidi et al
242   reported hepatitis in association with IgAN thus far have been in conjunction with viral infections
243   secondary to hepatitis A, B, and C [23]. Research indicated ALT, AST levels significantly increased in
244   the IgAN model group. In the present study, we found that endocapillary hypercellularity, tubular
245   atrophy, and interstitial fibrosis negatively affect renal survival. Furthermore, chronic lesions such as
246   tubulointerstitial fibrosis have been associated with poor prognosis in patients with IgAN[24-25]. To
247   date, the pathogenesis of IgAN, which often leads to sclerosis of the glomeruli, remains unclear.
248   Previous studies have suggested that proinflammatory cytokines such as IL-1β, IL-2, IL-4, IL-5, IL-6,
249   IL-8, and TNF-α may play an aggravating role in the development of inflammation and glomerular
250   damage in IgAN [26-29].

251   Toll-like receptors (TLRs) are key components of the mammalian innate immune system. TLRs
252   are known to be involved in the pathogenesis of various inflammatory diseases, including kidney
253   diseases such as ischemic acute kidney injury, organ transplant rejection, and immune-mediated
254   glomerulonephritis [30]. In the kidneys, TLR4 is expressed primarily in the proximal and distal
255   tubules and in Bowman's capsular epithelia [31-35], whereas minimal expression occurs in the
256   glomeruli and endothelial cells [36]. Under stress or inflammatory conditions, the expression of TLR4
257   is upregulated in various regions of the nephron [31,37]. Previous studies have shown that TLR4-
258   mediated upregulation of IL-6, IL-1β, and MCP-1 is significantly correlated TLR4 and MCP-1
259   expression. MCP-1 plays a central role in inflammation and causes tubulointerstitial lesions by
260   recruiting target cells, which include macrophages, monocytes, T cells, neutrophils, eosinophils, and
261   basophils, into the tubulointerstitium, where the target cells themselves secrete cytokines such as
262   TGF-β1 and TNF-α [38-39]. These have also shown that renal TLR4 expression is closely associated
263   with MCP-1, TGF-β1, and IL-6 expression, thereby suggesting that TLR4 plays a key role in chronic
264   renal pathophysiology. Patients with severe proteinuria show upregulated renal TLR4 expression,
265   thereby suggesting aggravation of inflammatory and fibrotic processes. Except for the inflammatory
266   response, oxidative stress causes the formation of reactive oxygen species, leading to renal injury[40].
267   TGF-β1 contributes to the development of tubulointerstitial fibrosis [41-42]. Furthermore, TGF-β1
268   secreted by mesangial and inflammatory cells in this model is closely involved in inflammatory
269   reactions and the accumulation of extracellular matrix [43-44]. Increased expression of the TGF-β1
270   gene is associated with glomerulosclerosis [45] and increased severity of tubulointerstitial damage.
271   The results of the present study show that high and low doses of periostracum cicadae can
272   dramatically decrease protein expression in the blood and urine in the rat models. Furthermore, high
273   doses of periostracum cicadae were determined to be more effective than low doses. Significant IgA
274   deposition in the glomeruli was also observed in these animals. These findings indicate the successful
275   establishment of an IgAN rat model. The results of the present study show a significant decrease in
276   serum IgA, TNF-α, IL-1β, and IL-6 levels, which in turn suppresses the growth of glomerular
277   mesangial cells and its extracellular matrix, improves IgAN symptoms, and protects renal function.
278   Immunohistochemical analysis indicated a larger TGF-β1-immunostained area in the glomeruli of
279   the IgAN models (Figure 6), which was significantly decreased after treatment with periostracum
280   cicadae at dose of 0.5 g/kg/day, 1.0 g/kg/day, and 2.0 g/kg/day. TLR4, IgA, and MCP-1 were
281   downregulated in the periostracum cicadae-treated rats compared to that in the IgAN animal models.
282   In conclusion, the present study has shown that the administration of periostracum cicadae improves
283   renal tissue inflammation and fibrotic processes.

284   Apoptosis of renal glomerular cells is known to contribute to the regulation of renal cell
285 proliferation, as well as induces the repair of damaged renal tissues. The degree of glomerular cell
286 apoptosis is commensurate with the decrease in the number of glomerular cells, accumulation in the
287 extracellular matrix, mesangial cell proliferation, and proteinuria in the progression of
288 glomerulosclerosis [46]. Fas, which is also known as apoptosis antigen-1 or cluster of differentiation
289 95, is a member of the death receptor family, a subfamily of the tumor necrosis factor receptor
290 superfamily [47]. Interactions between Fas and its natural ligand (Fas L) or agonistic antibodies
291 induce apoptosis in responsive cells [47]. Caspase-3 is a member of the cysteine-aspartic acid protease
292 (caspase)/IL-1β-converting enzyme family [48] and is directly activated by caspase-8, -9, and -10 via
293 extrinsic and intrinsic pathways that initiate apoptosis. Previous studies have revealed that caspase-
294 3 expression is positively associated with Fas and Fas L expression in human cells [49-50]. The present
295 study demonstrated that caspase-3 expression is correlated with Fas expression, similar to that
296 described in previous reports [49-51]. The present study also determined that Fas and caspase-3 are
297 upregulated in renal tissues as indicated by TUNEL staining and are associated with glomerular
298 injury. Furthermore, the number of Fas-positive cells and the expression of proteins involved in the
299 caspase-3 pathway in IgAN rats decreased relative to that in the saline-treated group. However, the
300 periostracum cicadae-treatment group showed an increase in the number of Fas-positive cells and
301 the levels of caspase-3 expression. Therefore, increased Fas and caspase-3 expression promoted
302 apoptosis in IgAN rat cells.

303   In summary, the pathological evaluation of kidney tissues indicates that rats treated with the
304 high doses of periostracum cicadae exhibit less kidney inflammation and fibrosis than the IgAN rats.
305 We also determined that the administration of periostracum cicadae significantly reduces TLR4, TGF-
306 β1, MCP-1, and IgA expression in the IgAN rats. The results of the present study also demonstrate
307 that the increase in the expression of Fas and its downstream signaling molecules such as caspase-3
308 may alleviate the symptoms of IgAN in patients.

309 **4. Materials and Methods**

310 *4.1. Reagents*

311   Enzyme-linked immunosorbent assay (ELISA) kits for rat TNF-α (Shanghai Xitang, Shanghai,
312 China), IL-6 (Shanghai Xitang), and IL-1β (Shanghai Xitang) were used according to the
313 manufacturer's instructions. Rabbit anti-TLR4 polyclonal antibody (Boster Biological Technology,
314 Pleasanton, CA, USA), rabbit anti-IgA polyclonal antibody, rabbit anti-MCP-1 polyclonal antibody
315 (Boster Biological Technology), and horseradish peroxidase (HRP)-labeled goat anti-rabbit IgG
316 antibody (Boster Biological Technology) were used in the detection of the corresponding target
317 proteins. Radioimmunoprecipitation assay (RIPA) lysis buffer (Solarbio Biological Technology,
318 Beijing, China), bicinchoninic acid (BCA) protein assay kit (Solarbio Biological Technology),
319 horseradish peroxidase (HRP)-conjugated secondary antibodies (Boster Biological Technology), and
320 an enhanced chemiluminescent (ECL) detection kit (Beyotime, Haimen, China) were also procured.

321 *4.2. Preparation of prednisone acetate extract*

322   Dried periostracum cicadae was purchased from a traditional medicine market in Xinjiang,
323 China and identified by Professor Jincai Lu of the School of Traditional Chinese Materia Medica of
324 Shenyang Pharmaceutical University. A voucher specimen (No. 20081001) was deposited in the
325 Research Department of Natural Medicine of Shenyang Pharmaceutical University. Dried
326 periostracum cicadae (5 kg) was refluxed three times with 70% ethanol (50 L) to obtain a crude extract.

327 *4.3. Animals*

328   One hundred and forty male SD rats (average weight: 140 ± 20 g) were obtained from the Animal
329 Center of Urumqi (Certificate No. SCXK [xin] 2011-0003, Urumqi, China). The SD rats were kept and

330 fed in a clean-grade room at a constant temperature (18°C) and humidity (45%) with a 12-h light/dark
331 cycle. Routine urine testing was performed after one week of pre-feeding using the test strip method.
332 Rats that showed no hematuria or proteinuria were selected and randomly distributed to each group.
333 All animal experiments were performed under institutionally approved protocols and complied with
334 the Guide for the Care and Use of Laboratory Animals.

335 *4.4. Establishment of a IgAN model*

336 The IgAN animal model, established based on the IgA nephropathy model and gavage of hot
337 drugs, was used to establish blood stasis and heat syndrome. The rats were randomly divided into
338 the following seven groups: untreated controls, IgAN model (IgAN group), prednisone acetate
339 control (PAG group, 6.3 mg/kg), tripterygium glycoside tablet control (9.4 mg/kg), and three groups
340 received oral periostracum cicadae (0.5 g/kg, 1 g/kg, and 2 g/kg). The rat IgAN model was established
341 by administering bovine serum albumin (BSA), lipopolysaccharide (LPS), and carbon tetrachloride
342 (CCl_4) as previously described [52-54], with slight modifications. Briefly, the immunogen BSA was
343 intragastrically administered at a dose of 4 mL/kg once every two days for eight consecutive weeks,
344 and 0.1 ml of CCl_4 in 0.3 mL of castor oil was given once weekly for nine weeks. On the 6th week of
345 treatment, 0.05 mg of LPS (Sigma, USA) was injected through the tail vein once every two weeks for
346 another six weeks to establish blood stasis and heat syndrome, symptoms that characterize the IgAN
347 model. On the 9th week, 25% ginger ale was intragastrically administered at a dose of 10 mL/kg once
348 every two days for 4 consecutive weeks. For the untreated control group, 4 mL/kg distilled water was
349 used instead of BSA, 0.4 mL of castor oil was employed to replace castor oil and CCl4, and saline was
350 used instead of LPS on the 6th week. The administration methods were the same as that in the model
351 group.

352 **Table 2.** Induction of IgAN in the SD rats

Control	BSA was replaced by distilled water; PBS was used as injection control	
IgAN	BSA,4 mL/kg	Intragastrically every 2 days for 8 weeks
	CCL$_4$/castor oil (25%, v/v)	S.c. injection,0.4 mL, once a week for 9 weeks
	LPS, 0.05 mg	Caudal i.v., once every two weeks for six weeks at the 6th week
	25% ginger ale, 10 mL/kg	Once every two days for four consecutive weeks on the 9th week

353 *4.5. Sample collection and preparation*

354 At the end of 16 weeks of treatment, 24-h urine samples was collected with metabolic cages, and
355 the model was identified based on the levels of 24-h urine protein, BUN, and serum creatinine (Scr).
356 Blood samples were obtained from the abdominal aorta upon sacrifice and were used in measuring
357 ALT, AST, TP, TCHO, TAG, BUN, and CREA using an automatic biochemistry analyzer.

358 In addition, rats from each group were sacrificed at different time points and their kidneys were
359 collected for histological examination. Each kidney was divided into three portions. The first portion
360 was fixed in 40 g/L formaldehyde, embedded in paraffin, cut into sections, and then stained with
361 eosin (H&E) and periodic acid-Schiff (PAS) for light microscopy. The second portion was embedded
362 in OTC and stored at −70°C, followed by frozen sectioning for immunofluorescence staining. The
363 third portion was stored at −70°C for western blotting

364 *4.6. Biochemical analysis of serum samples*

The blood samples were centrifuged at 1,500 rpm for 10 min at 4°C to isolate the serum, which was stored immediately at −80°C. Serum IgA, TNF-α, IL-1β, and IL-6 levels were determined using commercially available ELISA kits according to the manufacturer's instructions. The optical density value was determined using a microplate reader (Thermo Varioskan Flash 3001, USA) and calculated at the linear portion of the curve. The experiment was repeated thrice under the same conditions.

4.7. Histopathological examination

After blood collection, the kidneys were fixed in 10% (v/v) neutral formalin for 24 h. To enhance fixation, the kidneys were placed in a rubber-capped ampulla bottle that was 2/3 filled with 10% (v/v) neutral formalin and then vacuumed to allow complete immersion of the tissues. The kidney tissues were paraffin-embedded, sectioned (Leica, Nussloch, Germany) at a thickness of 5 μm, and stained with H&E for subsequent cell infiltration observation. Alternatively, sections were stained with PAS to examine mucus production. Quantitative analysis of mucus production was performed using Image-Pro Plus 6.0 (Media Cybernetics, Bethesda, MD, USA).

4.8. Immunofluorescence

The 5-μm thick frozen kidney sections were mounted on glass slides and air-dried. The tissue sections were stained with fluorescein isothiocyanate (FITC)-labelled polyclonal rabbit anti-IgA (diluted 1:10). IgA deposition was graded using a five-stage semi-quantitative method as follows: (−), no staining at low magnification and possible staining at high magnification; (+), possible staining at low magnification and staining at high magnification; (++), staining at low magnification and distinct staining at high magnification; (+++) distinct staining at low magnification and more intense staining at high magnification; and (++++), very intense staining at high magnification. In this study, most of the staining in the IgAN mode group ranged from ++ to +++.

4.9. TUNEL assay

The TUNEL staining kit was purchased from Roche (Basel, Switzerland). The staining procedure was as follows: (1) The tissue sections were deparaffinized by immersing the slides in xylene and rehydrated by sequentially immersing the slides across an ethanol gradient. (2) Endogenous peroxidase activity was quenched by adding 0.3% H_2O_2 for 10 min and then washed in 10 mmol/L PBS (pH 7.4) thrice for 5 min each. (3) The sections were digested with 20 μg/mL proteinase K for 25 min at room temperature and then washed in 10 mmol/L PBS (pH 7.4) thrice for 5 min each time. (4) The TUNEL reaction mixture was added to each section, followed by incubating in a humid chamber for 60 min at 37°C. (5) Then, the slides were washed in 10 mmol/L PBS (pH 7.4) thrice for 5 min each and incubated with peroxidase conjugated anti-flconjugate antibody in a humid chamber for 30 min at 37°C. The slides were then washed in 10 mmol/L PBS (pH 7.4) thrice for 5 min each time. (6) The tissue sections were stained with DAB for 5 min, counterstained with hematoxylin, dehydrated, cleared in xylene, and covered with a glass slip.

4.10. Immunohistochemical staining

The paraffin-embedded tissue sections were dewaxed, hydrated, treated with 5 mmol/L levamisole to block endogenous alkaline phosphatase, and incubated with blocking serum for 30 min at room temperature to reduce nonspecific background staining. The sections were rehydrated in phosphate-buffered saline/0.1% BSA for 15 min before addition of the appropriate blocking serum for an additional 15 min. The sections were incubated with polyclonal rabbit anti-TGF-β1 (dilution: 1:1,000; Chemicon, Temecula, CA, USA) and rabbit anti-FAS 15 g/mL (Santa Cruz Biotechnology, Santa Cruz, CA, USA) overnight at 4°C. The following day, the slides were rinsed, incubated with biotinylated goat anti-rabbit IgG (Abcam, UK) and then processed using an alkaline phosphatase-streptavidin-biotin immunoperoxidase method (Beijing Zhongshan Biotechnology Co., Ltd., China). The tissue sections were counterstained with hematoxylin. Negative controls for specific labeling were performed in parallel by replacing the primary antibody with normal rabbit serum. Renal cortex

412 sections were digitally imaged and quantitatively examined using a computer-assisted image
413 analysis software (CX41 light microscopy; Olympus). To quantitate the amount of chymase-positive
414 TGF-β1 and the area of FAS-positive expression in the tubulointerstitial compartment, 50 fields
415 consecutively selected in the cortical areas of the kidneys were examined at a magnification of 400×.
416 Fields containing glomeruli and large arteries were excluded. To quantitate the expression of TGF-
417 β1 and FAS in the tubulointerstitial compartment, the average percentage of positively staining
418 proportional area and the whole area was calculated by image analysis.

419 *4.11. Western blot analysis*

420 The nuclear and cytoplasmic proteins were extracted from the kidney tissues using an NE-PER
421 kit (Pierce Biotechnology, Rockford, IL, USA) according to the manufacturer's instructions. The
422 proteins were separated by sodium dodecyl sulfate-polyacrylamide gel electrophoresis and
423 transferred onto a polyvinylidene fluoride (PVDF) membrane (Millipore Corp., Billerica, MA, USA),
424 which was then incubated with an anti-TLR4 antibody (Cell Signaling Technology, Lexington, KY,
425 USA), an anti-IgA antibody (Cell Signaling Technology), an anti-caspase 3 antibody (Cell Signaling
426 Technology), an anti-MCP-1 antibody (Cell Signaling Technology) and anti-β-actin antibody (Cell
427 Signaling Technology) at 4°C overnight. After washing, the membrane was incubated with a
428 horseradish peroxidase-conjugated secondary antibody for 1 h. After washing five times with TBST,
429 the membranes were incubated with an HRP-conjugated antibody for 1 h at room temperature.
430 Western blots were developed using ECL (Thermo, NY, USA) and were exposed on Kodak
431 radiographic film.

432 *4.12. Statistical analysis*

433 Data were expressed as the mean ± SD of at least three independent experiments and evaluated
434 using ANOVA, followed by Bonferroni correction. $P < 0.05$ was considered statistically significant.
435 The analyses were performed using SPSS 17.0 statistical software program.

439 **Author Contributions:** For research articles with several authors, a short paragraph specifying their individual
440 contributions must be provided. The following statements should be used "Rena Kasimu and Lu Yang conceived
441 and designed the experiments; Aobulikasimu·Nuerbiye and Yan Wang performed the experiments; Yan Wang
442 analyzed the data; and Ping Cheng and Hong Li contributed reagents and materials tools."

443 **Conflicts of Interest:** The authors declare no conflicts of interest.

444 **References**

445 1. Hogg, R. J.; Wyatt, R. J. A randomized controlled trial of mycophenolate mofetil in patients with IgA
446   nephropathy. *BMC Nephrology* **2004**, 5, (1), 1-9.
447 2. Cai, G. Y; Chen, X. M. Immunoglobulin A nephropathy in China: progress and challenges. *Am J Nephrol*
448   **2009**, 30, (3), 268-273.
449 3. Kiryluk, K.; Julian, B. A.; Wyatt, R. J.; Scolari, F.; Zhang, H.; Novak, J.; Gharavi, A.G. Genetic studies of IgA
450   nephropathy: past, present, and future. *Pediatr Nephrol* **2010**, 25, (11), 2257-2268.
451 4. D'Amico, G. Natural history of idiopathic IgA nephropathy and factors predictive of disease outcome.
452   *Seminars in nephrology* **2004,** 24, (3), 179-196.
453 5. Boyd, J. K.; Cheung, C. K.; Molyneux, K.; Feehally, J.; Barratt, J. An update on the pathogenesis and
454   treatment of IgA nephropathy. *Kidney international* **2012,** 81, (9), 833-843.
455 6. Horie, A.; Hiki, Y.; Odani, H.; Yasuda, Y.; Takahashi, M.; Kato, M. IgA1 molecules produced by tonsillar
456   lymphocytes are under-O-glycosylated in IgA nephropathy. *Am J Kidney Dis* **2003**, 42(3), 486-96.
457 7. Ibels, L. S.; Gyory, A. Z.; Caterson, R. J.; Pollock, C. A.; Mahony, J. F.; Waugh, D. A. Primary iga
458   nephropathy: natural history and factors of importance in the progression of renal impairment. *Kidney*

459   *International Supplement* **1997**, 61(4), 67-70.

460   8.   Ohno, I.; Hosoya, T.; Gomi, H.; Ichida, K.; Okabe, H.; Hikita, M. Serum uric acid and renal prognosis in
461   patients with IgA nephropathy. *Nephron* **2001**, 87(4), 333-339.

462   9.   Barratt, J.; Feehally, J. IgA Nephropathy. *J Am Soc Nephrol* **2005**, 16, 2088-2097.

463   10.   Kim, C. H.; Lim, B. J.; Bae, Y. S.; Kwon, Y. E.; Kim, Y. L.; Nam, K. H.; Park, K. S.; An, S. Y.; Koo, H. M.; Doh,
464   F. M.; Lee, M. J.; Oh, H. J.; Yoo, T. H.; Kang, S. W.; Choi, K. H.; Jeong, H. J.; Han, S. H. Using the Oxford
465   classification of IgA nephropathy to predict long-term outcomes of Henoch-Schonlein purpura nephritis
466   in adults. *Modern pathology : an official journal of the United States and Canadian Academy of Pathology, Inc* **2014,**
467   27, (7), 972-982.

468   11.   Coppo, R.; Andrulli, S.; Amore, A.; Gianoglio, B.; Conti, G.; Peruzzi, L.; Locatelli, F.; Cagnoli, L. Predictors
469   of outcome in Henoch-Schonlein nephritis in children and adults. *American journal of kidney diseases : the*
470   *official journal of the National Kidney Foundation* **2006,** 47, (6), 993-1003.

471   12.   Bogdanovic, R. Henoch-Schonlein purpura nephritis in children: risk factors, prevention and treatment.
472   *Acta paediatrica (Oslo, Norway : 1992)* **2009,** 98, (12), 1882-1889.

473   13.   Roberts, I. S.; Cook, H. T.; Troyanov, S.; Alpers, C. E.; Amore, A.; Barratt, J.; Berthoux, F.; Bonsib, S.; Bruijn,
474   J. A.; Cattran, D. C.; Coppo, R.; D'Agati, V.; D'Amico, G.; Emancipator, S.; Emma, F.; Feehally, J.; Ferrario,
475   F.; Fervenza, F. C.; Florquin, S.; Fogo, A.; Geddes, C. C.; Groene, H. J.; Haas, M.; Herzenberg, A. M.; Hill, P.
476   A.; Hogg, R. J.; Hsu, S. I.; Jennette, J. C.; Joh, K.; Julian, B. A.; Kawamura, T.; Lai, F. M.; Li, L. S.; Li, P. K.;
477   Liu, Z. H.; Mackinnon, B.; Mezzano, S.; Schena, F. P.; Tomino, Y.; Walker, P. D.; Wang, H.; Weening, J. J.;
478   Yoshikawa, N.; Zhang, H. The Oxford classification of IgA nephropathy: pathology definitions, correlations,
479   and reproducibility. *Kidney international* **2009,** 76, (5), 546-556.

480   14.   Coppo, R.; Troyanov, S.; Camilla, R.; Hogg, R. J.; Cattran, D. C.; Cook, H. T.; Feehally, J.; Roberts, I. S.;
481   Amore, A.; Alpers, C. E.; Barratt, J.; Berthoux, F.; Bonsib, S.; Bruijn, J. A.; D'Agati, V.; D'Amico, G.;
482   Emancipator, S. N.; Emma, F.; Ferrario, F.; Fervenza, F. C.; Florquin, S.; Fogo, A. B.; Geddes, C. C.; Groene,
483   H. J.; Haas, M.; Herzenberg, A. M.; Hill, P. A.; Hsu, S. I.; Jennette, J. C.; Joh, K.; Julian, B. A.; Kawamura, T.;
484   Lai, F. M.; Li, L. S.; Li, P. K.; Liu, Z. H.; Mezzano, S.; Schena, F. P.; Tomino, Y.; Walker, P. D.; Wang, H.;
485   Weening, J. J.; Yoshikawa, N.; Zhang, H. The Oxford IgA nephropathy clinicopathological classification is
486   valid for children as well as adults. *Kidney international* **2010,** 77, (10), 921-927.

487   15.   Alamartine, E.; Sauron, C.; Laurent, B.; Sury, A.; Seffert, A.; Mariat, C. The use of the Oxford classification
488   of IgA nephropathy to predict renal survival. *Clinical journal of the American Society of Nephrology : CJASN*
489   **2011,** 6, (10), 2384-2388.

490   16.   Herzenberg, A. M.; Fogo, A. B.; Reich, H. N.; Troyanov, S.; Bavbek, N.; Massat, A. E.; Hunley, T. E.;
491   Hladunewich, M. A.; Julian, B. A.; Fervenza, F. C.; Cattran, D. C. Validation of the Oxford classification of
492   IgA nephropathy. *Kidney international* **2011,** 80, (3), 310-317.

493   17.   Katafuchi, R.; Ninomiya, T.; Nagata, M.; Mitsuiki, K.; Hirakata, H. Validation study of oxford classification
494   of IgA nephropathy: the significance of extracapillary proliferation. *Clinical journal of the American Society of*
495   *Nephrology : CJASN* **2011,** 6, (12), 2806-2813.

496   18.   Shi, S. F.; Wang, S. X.; Jiang, L.; Lv, J. C.; Liu, L. J.; Chen, Y. Q.; Zhu, S. N.; Liu, G.; Zou, W. Z.; Zhang, H.;
497   Wang, H. Y. Pathologic predictors of renal outcome and therapeutic efficacy in IgA nephropathy: validation
498   of the oxford classification. *Clinical journal of the American Society of Nephrology : CJASN* **2011,** 6, (9), 2175-
499   2184.

500   19.   Hsieh, M. T.; Peng, W. H.; Yeh, F. T.; Tsai, H. Y.; Chang, Y. S. Studies on the anticonvulsive, sedative and
501   hypothermic effects of Periostracum Cicadae extracts. *Journal of ethnopharmacology* **1991,** 35, (1), 83-90.

502   20.   Xu, M. Z.; Lee, W. S.; Han, J. M.; Oh, H. W.; Park, D. S.; Tian, G. R.; Jeong, T. S.; Park, H. Y. Antioxidant and
503   anti-inflammatory activities of N-acetyldopamine dimers from Periostracum Cicadae. *Bioorganic &*
504   *medicinal chemistry* **2006,** 14, (23), 7826-7834.

505   21.   Noda, N.; Kubota, S.; Miyata, Y.; Miyahara, K. Optically active N-acetyldopamine dimer of the crude drug
506   "Zentai," the cast-off shell of the Cicada, Cryptotympana sp. *Chemical & pharmaceutical bulletin* **2000,** 48, (11),
507   1749-1752.

508   22.   Shin, T. Y.; Park, J. H.; Kim, H. M. Effect of Cryptotympana atrata extract on compound 48/80-induced
509   anaphylactic reactions. *Journal of ethnopharmacology* **1999,** 66, (3), 319-325.

510   23.   Zaidi, M.; Singh, N.; Kamran, M.; Ansari, N.; Nasr, S. H.; Acharya, A. Acute onset of hematuria and
511   proteinuria associated with multiorgan involvement of the heart, liver, pancreas, kidneys, and skin in a
512   patient with Henoch-Schönlein purpura. *Kidney International* **2008**, 73, (4), 503-508.

513 24. Shrestha, S.; Sumingan, N.; Tan, J.; Alhous, H.; McWilliam, L.; Ballardie, F. Henoch Schonlein purpura with
514   nephritis in adults: adverse prognostic indicators in a UK population. *QJM : monthly journal of the Association*
515   *of Physicians* **2006,** 99, (4), 253-265.

516 25. Szeto, C. C.; Choi, P. C.; To, K. F.; Li, P. K.; Hui, J.; Chow, K. M.; Leung, C. B.; Lui, S. F.; Mac-Moune Lai, F.
517   Grading of acute and chronic renal lesions in Henoch-Schonlein purpura. *Modern pathology : an official*
518   *journal of the United States and Canadian Academy of Pathology, Inc* **2001,** 14, (7), 635-640.

519 26. Wu, T. H.; Wu, S. C.; Huang, T. P.; Yu, C. L.; Tsai, C. Y. Increased excretion of tumor necrosis factor alpha
520   and interleukin 1 beta in urine from patients with IgA nephropathy and Schonlein-Henoch purpura.
521   *Nephron* **1996,** 74, (1), 79-88.

522 27. Hirayama, K.; Kobayashi, M.; Muro, K.; Yoh, K.; Yamagata, K.; Koyama, A. Specific T-cell receptor usage
523   with cytokinemia in Henoch-Schonlein purpura nephritis associated with Staphylococcus aureus infection.
524   *Journal of internal medicine* **2001,** 249, (4), 289-295.

525 28. Nakajima, M.; Kawahara, S.; Sakagami, Y.; Takagawa, K.; Akazawa, H.; Kamitsuji, H.; Yoshioka, A.
526   Immunogold labelling of cytokines in glomeruli in children with various renal diseases. *Nephron* **1999,** 83,
527   (2), 132-138.

528 29. Kawasaki, Y.; Hosoya, M.; Suzuki, H. Possible pathogenic role of interleukin-5 and eosino cationic protein
529   in Henoch-Schonlein purpura nephritis. *Pediatrics international : official journal of the Japan Pediatric Society*
530   **2005,** 47, (5), 512-517.

531 30. Michalska, M.; Gluba, A.; Mikhailidis, D. P.; Nowak, P.; Bielecka-Dabrowa, A.; Rysz, J.; Banach, M. The role
532   of polyphenols in cardiovascular disease. *Medical science monitor : international medical journal of experimental*
533   *and clinical research* **2010,** 16, (5), Ra110-119.

534 31. El-Achkar, T. M.; Huang, X.; Plotkin, Z.; Sandoval, R. M.; Rhodes, G. J.; Dagher, P. C. Sepsis induces changes
535   in the expression and distribution of Toll-like receptor 4 in the rat kidney. *American journal of physiology.*
536   *Renal physiology* **2006,** 290, (5), F1034-1043.

537 32. Zager, R. A.; Johnson, A. C.; Lund, S.; Randolph-Habecker, J. Toll-like receptor (TLR4) shedding and
538   depletion: acute proximal tubular cell responses to hypoxic and toxic injury. *American journal of physiology.*
539   *Renal physiology* **2007,** 292, (1), F304-312.

540 33. Patole, P. S.; Pawar, R. D.; Lech, M.; Zecher, D.; Schmidt, H.; Segerer, S.; Ellwart, A.; Henger, A.; Kretzler,
541   M.; Anders, H. J. Expression and regulation of Toll-like receptors in lupus-like immune complex
542   glomerulonephritis of MRL-Fas(lpr) mice. *Nephrology, dialysis, transplantation : official publication of the*
543   *European Dialysis and Transplant Association - European Renal Association* **2006,** 21, (11), 3062-3073.

544 34. Tsuboi, N.; Yoshikai, Y.; Matsuo, S.; Kikuchi, T.; Iwami, K.; Nagai, Y.; Takeuchi, O.; Akira, S.; Matsuguchi,
545   T. Roles of toll-like receptors in C-C chemokine production by renal tubular epithelial cells. *Journal of*
546   *immunology (Baltimore, Md. : 1950)* **2002,** 169, (4), 2026-2033.

547 35. Samuelsson, P.; Hang, L.; Wullt, B.; Irjala, H.; Svanborg, C. Toll-like receptor 4 expression and cytokine
548   responses in the human urinary tract mucosa. *Infection and immunity* **2004,** 72, (6), 3179-3186.

549 36. Wolfs, T. G.; Buurman, W. A.; van Schadewijk, A.; de Vries, B.; Daemen, M. A.; Hiemstra, P. S.; van 't Veer,
550   C. In vivo expression of Toll-like receptor 2 and 4 by renal epithelial cells: IFN-gamma and TNF-alpha
551   mediated up-regulation during inflammation. *Journal of immunology (Baltimore, Md. : 1950)* **2002,** 168, (3),
552   1286-1293.

553 37. El-Achkar, T. M.; Wu, X. R.; Rauchman, M.; McCracken, R.; Kiefer, S.; Dagher, P. C. Tamm-Horsfall protein
554   protects the kidney from ischemic injury by decreasing inflammation and altering TLR4 expression.
555   *American journal of physiology. Renal physiology* **2008,** 295, (2), F534-544.

556 38. Wang, W. M.; Zhang, H. D.; Jin, Y. M.; Zhu, B. B.; Chen, N. PPAR-gamma agonists inhibit TGF-beta1-
557   induced chemokine expression in human tubular epithelial cells. *Acta pharmacologica Sinica* **2009,** 30, (1),
558   107-112.

559 39. Li, H.; Ruan, X. Z.; Powis, S. H.; Fernando, R.; Mon, W. Y.; Wheeler, D. C.; Moorhead, J. F.; Varghese, Z.
560   EPA and DHA reduce LPS-induced inflammation responses in HK-2 cells: evidence for a PPAR-gamma-
561   dependent mechanism. *Kidney international* **2005,** 67, (3), 867-874.

562 40. Hosohata K. Role of Oxidative Stress in Drug-Induced Kidney Injury. *International Journal of Molecular*
563   *Sciences* **2016**, 17(11), 1826.

564 41. Hwang, M.; Kim, H. J.; Noh, H. J.; Chang, Y. C.; Chae, Y. M.; Kim, K. H.; Jeon, J. P.; Lee, T. S.; Oh, H. K.; Lee,
565   Y. S.; Park, K. K. TGF-beta1 siRNA suppresses the tubulointerstitial fibrosis in the kidney of ureteral
566   obstruction. *Experimental and molecular pathology* **2006,** 81, (1), 48-54.

42. Murphy, M.; Docherty, N. G.; Griffin, B.; Howlin, J.; McArdle, E.; McMahon, R.; Schmid, H.; Kretzler, M.; Droguett, A.; Mezzano, S.; Brady, H. R.; Furlong, F.; Godson, C.; Martin, F. IHG-1 amplifies TGF-beta1 signaling and is increased in renal fibrosis. *Journal of the American Society of Nephrology : JASN* **2008,** 19, (9), 1672-1680.

43. Yu, L.; Border, W. A.; Anderson, I.; McCourt, M.; Huang, Y.; Noble, N. A. Combining TGF-beta inhibition and angiotensin II blockade results in enhanced antifibrotic effect. *Kidney international* **2004,** 66, (5), 1774-1784.

44. Martini, S.; Kramer, S.; Loof, T.; Wang-Rosenke, Y.; Daig, U.; Budde, K.; Neumayer, H. H.; Peters, H. S1P modulator FTY720 limits matrix expansion in acute anti-thy1 mesangioproliferative glomerulonephritis. *American journal of physiology. Renal physiology* **2007,** 292, (6), F1761-1770.

45. Yang, C. W.; Hsueh, S.; Wu, M. S.; Lai, P. C.; Huang, J. Y.; Wu, C. H.; Hu, S. A.; Chen, J. F.; Huang, C. C. Glomerular transforming growth factor-beta1 mRNA as a marker of glomerulosclerosis-application in renal biopsies. *Nephron* **1997,** 77, (3), 290-297.

46. Sugiyama, H.; Kashihara, N.; Makino, H.; Yamasaki, Y.; Ota, A. Apoptosis in glomerular sclerosis. *Kidney international* **1996,** 49, (1), 103-111.

47. Neumann, L.; Pforr, C.; Beaudouin, J.; Pappa, A.; Fricker, N.; Krammer, P. H.; Lavrik, I. N.; Eils, R. Dynamics within the CD95 death-inducing signaling complex decide life and death of cells. *Molecular systems biology* **2010,** 6, 352.

48. Medema, J. P.; Scaffidi, C.; Kischkel, F. C.; Shevchenko, A.; Mann, M.; Krammer, P. H.; Peter, M. E. FLICE is activated by association with the CD95 death-inducing signaling complex (DISC). *The EMBO journal* **1997,** 16, (10), 2794-2804.

49. Zheng, H. C.; Sun, J. M.; Wei, Z. L.; Yang, X. F.; Zhang, Y. C.; Xin, Y. Expression of Fas ligand and caspase-3 contributes to formation of immune escape in gastric cancer. *World journal of gastroenterology* **2003,** 9, (7), 1415-1420.

50. Nho, R. S.; Peterson, M.; Hergert, P.; Henke, C. A. FoxO3a (Forkhead Box O3a) deficiency protects Idiopathic Pulmonary Fibrosis (IPF) fibroblasts from type I polymerized collagen matrix-induced apoptosis via caveolin-1 (cav-1) and Fas. *PloS one* **2013,** 8, (4), e61017.

51. Ran, X.; Diao, J. X. Huangzhi Oral Liquid Prevents Arrhythmias by Upregulating Caspase-3 and Apoptosis Network Proteins in Myocardial Ischemia-Reperfusion Injury in Rats. *Evidence-Based Complementray and Alternative Medicine* **2015,** 518926.

52. Tang, Y.; Lou, T. Q.; Cheng, C. L.The modification of laboratory IgA nephropathy model. *J Zhongshan Univ (Med)* **2006,** 27, 184-187.

53. Peng, W.; Liu, Z. R. Comparison of two rat models of IgA nephropathy. *J South Med Univ* **2008,** 28,   1842-1845.

54. Lu, H.; Chen, L. L.; Jiang, X. Y.; Sun, L. Z. Temporal and spatial expression of podocyte-associated molecules are accompanied by proteinuria in IgA nephropathy rat model. *Physiological Research* **2013,** 62(1), 35-45.